

# Tumour tissue selectivity in the uptake and retention of SN 28049, a new topoisomerase II-directed anticancer agent

Pradeep B. Lukka · Ying Yi Chen · Graeme J. Finlay ·  
Wayne R. Joseph · Emma Richardson ·  
James W. Paxton · Bruce C. Baguley

Received: 14 May 2013 / Accepted: 27 August 2013 / Published online: 14 September 2013  
© Springer-Verlag Berlin Heidelberg 2013

## Abstract

**Purpose** A variety of anticancer drugs, including doxorubicin and mitoxantrone, have structures in which a DNA-intercalating chromophore is linked to a positively charged side chain. These drugs generally inhibit tumour growth and survival by poisoning the enzyme DNA topoisomerase II. SN 28049, a benzonaphthyridine derivative with these properties, has curative activity against the Colon 38 tumour in mice. Previous pharmacokinetic studies have demonstrated tumour-selective retention with approximately 20-fold higher area under the concentration–time curve (AUC) for tumour tissue as compared to normal tissues. We have investigated here whether such retention is tumour specific.

**Methods** Plasma and tissue pharmacokinetics were assessed in the murine Lewis lung (LL3) tumour in C57 BL/6 mice and in xenografts of the NZM4, NZM10 and NZM52 human melanoma lines in Balb/c Rag-1 immunodeficient mice. The in vitro cellular localisation of SN 28049 in murine and human cell lines was studied by confocal fluorescence microscopy.

**Results** A 260-fold variation, from 8.9  $\mu\text{M h}$  (NZM4) to 2,334  $\mu\text{M h}$  (Colon 38), was found among the different tumours. Only small variations were observed in the

corresponding plasma AUC (2.9–5  $\mu\text{M h}$ ). Moreover, in vivo activity, as measured by tumour growth delay, varied from 1 day (NZM4) to curative (Colon 38), consistent with the tumour pharmacokinetic data. In cultured cell lines, SN 28049 was found in cytoplasmic bodies, suggesting that drug sequestration could contribute to tumour pharmacokinetics.

**Conclusion** SN 28049 shows dramatic differences in both tumour AUC and antitumour activity against different tumours. These differences point to the presence of a tumour-specific uptake and retention mechanism.

**Keywords** Antitumour · Benzonaphthyridine · Topoisomerase poison · Xenograft · Pharmacokinetics · Confocal microscopy

## Introduction

DNA-intercalating compounds that poison the action of the enzyme topoisomerase II, causing it to induce DNA double-stranded breaks, have provided a rich source of experimental and clinical anticancer drugs. Amsacrine [1] and doxorubicin [2] were among the first such drugs to be characterised, but their discovery also raised important questions about tumour selectivity. Doxorubicin was active against a variety of carcinomas [3], but daunorubicin, a structurally highly similar congener, had a narrower spectrum of clinical activity encompassing mainly leukaemias. The basis for this difference in antitumour spectrum is not known, but an important clue was provided by pharmacokinetic studies of anthracycline derivatives, in which doxorubicin was found to be taken up more effectively than daunorubicin by the murine Lewis lung tumour, particularly at early times, and was also more active against this tumour

P. B. Lukka · Y. Y. Chen · G. J. Finlay · W. R. Joseph ·  
E. Richardson · B. C. Baguley (✉)  
Auckland Cancer Society Research Centre, Faculty of Medical  
and Health Sciences, The University of Auckland, Private Bag  
92019, Auckland 1142, New Zealand  
e-mail: b.baguley@auckland.ac.nz

P. B. Lukka · J. W. Paxton  
Department of Pharmacology and Clinical Pharmacology,  
The University of Auckland, Private Bag 92019, Auckland,  
New Zealand

[4]. This result suggested that differences in tumour tissue pharmacokinetics might be responsible for differences in antitumour activity.

The acridine derivative amsacrine is a synthetic topoisomerase II poison and its clinical activity, like that of daunorubicin, is restricted mainly to leukaemia [5]. Analogues of amsacrine, as well as structurally related drugs that include a DNA-intercalating chromophore attached to a positively charged side chain, have been synthesised with the aim of developing broader clinical activity [6, 7]. In the course of testing these drugs, some benzonaphthyridine derivatives, including the drug SN 28049 (structure in Fig. 1), were found to have outstanding activity against the murine Colon 38 tumour [8–10]. In vitro assessment of SN 28049 was carried out using a murine Colon 38 tumour cell line and the human HCT116 colon tumour line [11], but did not produce a clear explanation for the observed high in vivo activity in comparison with other DNA-binding drugs [12]. However, a pharmacokinetic study in mice with subcutaneously implanted Colon 38 tumours demonstrated selective and sustained retention of SN 28049 in tumour tissue [13]. The chromophore of SN 28049 differs from that of earlier DNA-binding drugs in having a methyl-substituted ring amide (Fig. 1), raising the question of whether this motif contributes in some way to its high solid tumour activity. We therefore compared the pharmacokinetics of a homologous series of benzonaphthyridine derivatives in which the amide methyl group was replaced by hydrogen, ethyl, propyl or butyl. This study showed that small structural changes resulted in large differences in tumour retention; for instance, changing the methyl group on the ring amide to hydrogen decreased the area under the concentration–time curve (AUC) in Colon 38 tumour tissue by 89-fold, and changing it to an ethyl group decreased the AUC by 10-fold [14]. These structural alterations also decreased antitumour activity in vitro and in vivo but had little effect on DNA-binding properties.

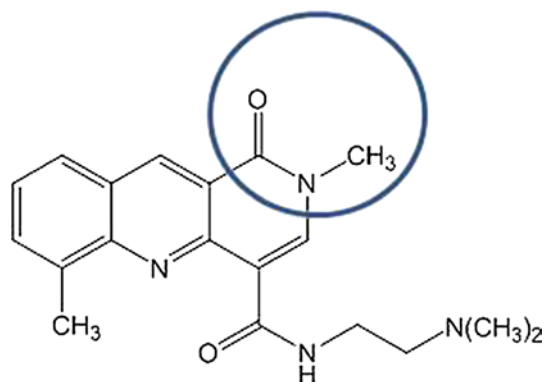


**Fig. 1** Structure of SN 28049. The *circle* shows the cyclic amide region

The results showed some similarity to the earlier data with doxorubicin and daunorubicin, where a small structural change affected both in vivo activity and in vivo pharmacokinetics [4].

An important question arising from the studies with SN 28049 is whether the high degree of SN 28049 retention observed in Colon 38 tissue is tumour specific. In this report, we have compared plasma, normal tissue and tumour tissue pharmacokinetics for Colon 38 with that for another murine tumour, Lewis lung, as well as for three human melanoma cell lines, grown as xenografts in immunodeficient mice. We have also measured tumour growth delays induced by SN 28049 in these tumours and determined whether they are related to drug retention. Finally, we have compared the subcellular distribution of SN 28049 in cultured, unfixed cells using fluorescence microscopy.

## Materials and methods

### Tumour cell lines

The Colon 38 tumour was obtained in 1981 from the Mason Research Institute, Worcester, MA, USA, and the Lewis lung tumour was obtained in 1977 from the Developmental Therapeutics Program of the National Cancer Institute. Both were maintained as transplanted subcutaneous tumours as described in [15]. The Co38P cell line was derived from the in vivo Colon 38 tumour as described in [11], while the LLTC cell line, obtained from Dr. R.C. Jackson (Warner-Lambert Company, Ann Arbor, MI, USA), had been developed from the in vivo Lewis lung tumour at the Southern Research Institute, Birmingham, AL, USA [16]. The NZM4, NZM10 and NZM52 melanoma cell lines were cultured from clinical samples from patients with metastatic melanoma as described in [17–19]. The Co38P and LLTC cell lines were maintained in  $\alpha$ -modified minimal essential medium ( $\alpha$ MEM) (Gibco Life Technologies, Grand Island, NY, USA) supplemented with 100 units/mL of penicillin, 100  $\mu$ g/mL of streptomycin (Sigma-Aldrich, St Louis, MO, USA) and 10 % foetal bovine serum (FBS) and grown at 37 °C in humidified conditions and 5 % CO<sub>2</sub>. The NZM cell lines were maintained in  $\alpha$ MEM supplemented with insulin (5  $\mu$ g/mL), transferrin (5  $\mu$ g/mL) and sodium selenite (5 ng/mL) (Roche Applied Sciences, Penzberg, Germany), 100 units/mL of penicillin, 100  $\mu$ g/mL of streptomycin and 5 % FBS and were grown under low (5 %) oxygen conditions.

### Tumour inoculation in mice

C57 BL/6 female mice were used for the inoculation of Lewis lung, LLTC and Colon 38 tumours, while

immunodeficient Balb/c Rag-1 female mice were used for inoculation of the human melanoma lines (NZM4, NZM10 and NZM52). All experimental procedures, including blood collection in mice from the ocular sinus under isoflurane anaesthesia, were approved by the University of Auckland Animal Ethics Committee and conformed to the Guidelines for the Welfare of Animals in Experimental Neoplasia, as set out by the United Kingdom Co-ordinating Committee on Cancer Research [20]. The *in vivo* Colon 38 and Lewis lung cell lines were transplanted subcutaneously as described in [15] except that C57 BL/6 recipient mice were used. Cultured cell lines were grown in tissue culture flasks, recovered using 0.05 % trypsin (Gibco Life Technologies, Grand Island, NY, USA) in phosphate buffered saline (PBS), collected by centrifugation and the cell density quantitated using a Coulter counter. The growth medium was replaced by medium without FBS and adjusted to give a cellular concentration of  $10^8$  cells/mL. A 100  $\mu$ L aliquot was injected subcutaneously into each mouse.

#### Formulation and dosing

SN 28049 as the free base (99 % pure by liquid chromatography; MW 338) was synthesised in the Auckland Cancer Society Research Centre using published methods [8]. It was dissolved in PBS and injected intraperitoneally (i.p.) into female tumour-bearing mice ( $n = 3$  per time point) at a dose of 17.4 (Balb/c Rag-1 mice) or 25  $\mu$ mol/kg (C57 BL/6 mice) (10  $\mu$ L/g of body weight). This lower dose (17.4  $\mu$ mol/kg) was the maximum tolerated dose in Rag-1 mice. For reasons of economy, pharmacokinetic experiments were carried out in tumour-bearing but not in non-tumour-bearing mice.

#### Analysis of mouse plasma and tissue homogenates

Experiments were carried out when tumour volumes reached 0.3–0.5 ml, 15–20 days after inoculation. Blood and tissues (heart, kidney, liver and tumour) were collected from anaesthetised mice at various time points after drug administration up to 72 h (0.08, 0.5, 1, 2, 4, 8, 12, 24, 48 and 72 h) from C57 BL/6 mice with LLTC tumours and up to 24 h (1, 4 and 24 h) for the tumour xenografts ( $n = 3$  mice per time point). Fewer time points were chosen for the latter due to limited supply of Balb/c Rag-1 mice. Plasma was separated from blood by centrifugation, and tissues, after washing with PBS, were homogenised in PBS. Samples were deproteinised and drug concentrations were measured using a validated LC–MS/MS method as described in [21].

#### Liquid chromatography–mass spectrometry (LC–MS/MS) analysis

The analyte and its deuterated internal standard ( $d_7$ ) were measured using a validated LC–MS/MS assay [21]. Samples (plasma and tissues) were deproteinised with 3 volumes of ice-cold acetonitrile:methanol (3:1). The organic phase was separated by centrifugation ( $13,000 \times g$ , 5 min) and diluted (1:1) in mobile phase (0.01 % formic acid in water) prior to injection into the LC–MS/MS. The LC–MS/MS system was an Agilent 1200 Rapid Resolution HPLC and Agilent 6410 triple quadrupole mass spectrometer equipped with a multimode ionisation source (Agilent Technologies, Santa Clara, CA, USA). Analytes were chromatographically separated using an Agilent Zorbax SB-C18 ( $50 \times 2.1$  mm, 5  $\mu$ m) column. A gradient elution (flow rate 0.5 mL/min) was employed with a run time of 7 min per sample. The assay had a lower limit of quantitation (LLOQ) of 1 nM and was linear from 1 to 300 nM. Validation using plasma and mouse tissues showed acceptable intra- and inter-assay precision (<7.1 %; <6.5 %), intra-assay accuracy ( $92.1 \pm 5.5$  %) and inter-assay accuracy ( $102.1 \pm 5.5$  %).

#### Pharmacokinetic data analysis

Concentration–time courses for plasma and tissues were fitted to a non-compartmental model using Phoenix WinNonlin (Pharsight, Sunnyvale, CA, USA). Area under the concentration–time curve was calculated by the log trapezoidal rule with extrapolation of the terminal slope to infinity by log-linear regression (AUC  $0-\infty$ ).  $C_{\max}$  (maximum concentration achieved) was derived and the elimination half-life ( $t_{1/2}$ ) and calculated from the equation  $t_{1/2} = \ln(2)/\lambda_Z$ , where  $\lambda_Z$  is the rate constant associated with the terminal elimination phase for concentration data. The model-independent pharmacokinetic parameters, clearance (CL) and volume of distribution at steady state ( $V_{SS}$ ), were calculated by the equations  $CL = F \times \text{Dose}/\text{AUC}$ ;  $V_{SS} = (F \times \text{Dose} \times \text{AUMC})/(\text{AUC})^2$ , where AUMC represents the total area under the first moment of the concentration–time curve, computed in a similar fashion to that used for AUC, and F is the bioavailability after i.p. administration. Results were expressed as mean  $\pm$  SEM. The statistical differences between the groups were calculated using two-way ANOVA by SigmaPlot 11 (Systat Software Inc., San Jose, CA, USA).  $p$  values of <0.05 were considered significant.

#### Tumour growth delay experiments

Experiments were carried out as described in [15] with treatment initiated when tumour diameters were 3–4 mm

(Colon 38 and Lewis lung), 4–5 mm (NZM4 and NZM52) or 3–5 mm (NZM10). Tumour diameters were measured with callipers three times weekly and volumes calculated as  $0.52 \times a^2 \times b$ , where  $a$  and  $b$  are the minor and major tumour axes. Mean tumour diameters in these experiments did not exceed 12 mm, as recommended by guidelines [20].

#### Confocal microscopy of drug distribution in cultured cells

Cells were incubated for 1 h with SN 28049 (10  $\mu\text{M}$ ) at 37 °C under humidified conditions. Growth medium was removed, and plates were washed three times with PBS supplemented with 10 % FBS and then re-suspended in PBS. Fluorescent images of live cells were obtained using a confocal laser scanning microscope (Leica TCS SP2; Leica Microsystems, Wetzlar, Germany) fitted with a water immersion UV objective with a numerical aperture of 0.9 (HCX APO L 63  $\times$  0.9 W UV). SN 28049 fluorescence emission was detected 400–586 nm with UV laser excitation at 351 nm/364 nm. Transmitted light images were

captured using the same objective. Images were acquired and processed using the Leica Confocal Software (LCS) version 2.61.

## Results

#### Comparison of SN 28049 pharmacokinetics in murine tumours

Plasma and tissue pharmacokinetic data for Lewis lung tumour-bearing mice are shown in Fig. 2. Plasma, heart, kidney, liver and tumour pharmacokinetics are presented and compared with published data for Colon 38 tumour-bearing mice [14], in Tables 1 and 2. The tumour AUC for Lewis lung (217  $\mu\text{M h}$ ) was less than one-tenth of that for Colon 38 (2,334  $\mu\text{M h}$ ) even though the plasma AUC values were similar. It was of interest that the AUC values for heart and liver tissue (but not kidney) in mice with Lewis lung tumours were significantly higher ( $p < 0.001$ ) than the corresponding values for mice with Colon 38 tumours.

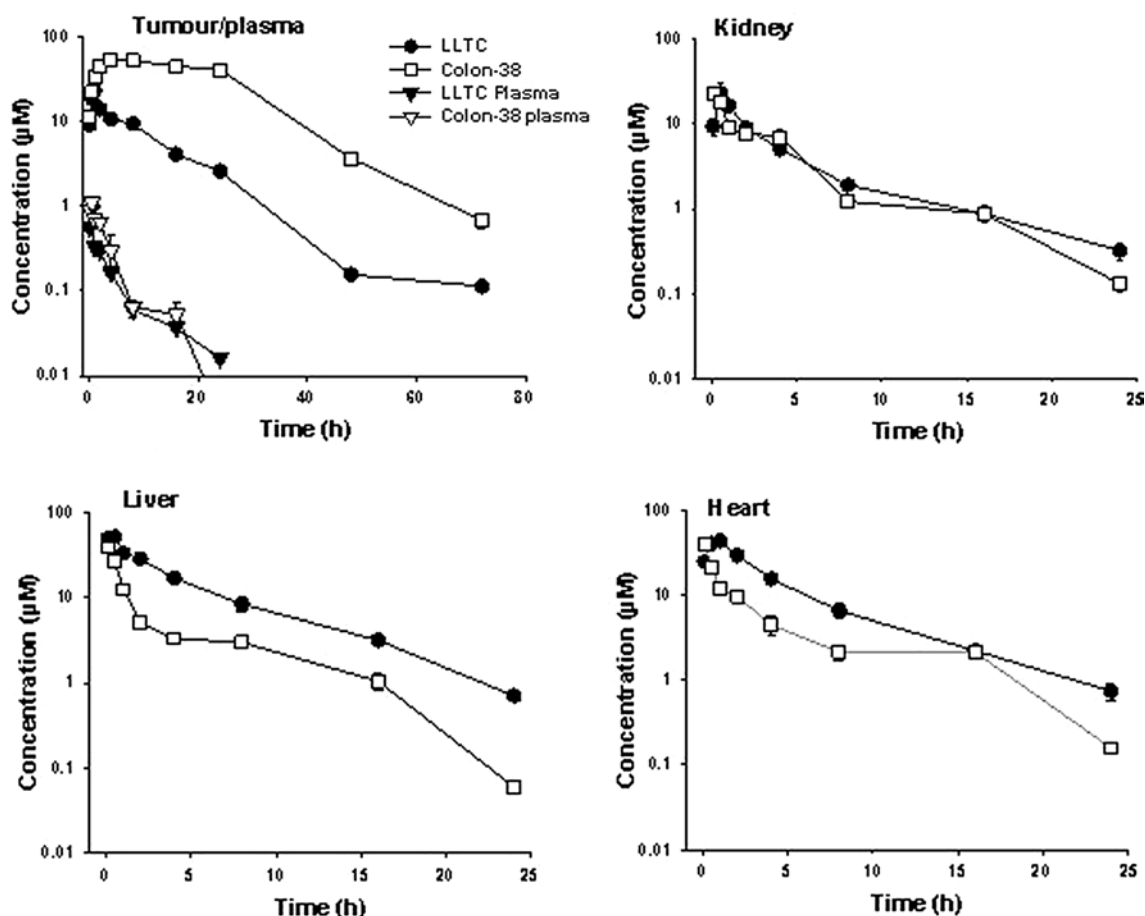


**Fig. 2** Tissue concentrations of SN 28049 (mean  $\pm$  SEM) for tumour, plasma, kidney, liver and heart after i.p. drug administration (25  $\mu\text{mol/kg}$ ) to tumour-bearing C57 BL/6 female mice ( $n = 3$  per time point)

**Table 1** Plasma pharmacokinetic parameters calculated from concentration–time profiles after i.p. administration of SN 28049 to C57 BL/6 (25 µmol/kg) or Balb/c Rag-1(17.4 µmol/kg) tumour-bearing female mice ( $n = 3$  per time point)

Host	Tumour	AUC (0–∞) (µM h)	$C_{max}$ (µM)	$t_{1/2}$ (h)	CL/F (l/h/kg)	V <sub>ss</sub> /F (l/kg)
C57 BL6 <sup>a</sup>	None	2.8 ± 0.2	0.6 ± 0.01	3.2 ± 0.04	9.3 ± 0.5	42.6 ± 2.6
C57 BL6	LLTC	2.7 ± 0.02	0.9 ± 0.05	4.6 ± 0.4	10.3 ± 0.1	96.5 ± 4.6
C57 BL6 <sup>a</sup>	Colon 38	2.9 ± 0.2	0.6 ± 0.01	3.2 ± 0.1	9.3 ± 0.5	42.3 ± 2.6
Rag-1	NZM4	3.3 ± 0.2	0.4 ± 0.02	3.3 ± 0.5	5.3 ± 0.3	24.9 ± 3.4
Rag-1	NZM10	4.0 ± 0.3	0.6 ± 0.03	3.7 ± 0.2	4.7 ± 0.3	24.3 ± 1.1
Rag-1	NZM52	5.0 ± 0.1	0.6 ± 0.03	3.3 ± 0.2	3.5 ± 0.1	16.7 ± 1.0

Values are expressed as mean ± SEM

<sup>a</sup> From published data [21]

**Table 2** Tissue pharmacokinetic parameters calculated from concentration–time profiles after i.p. administration of SN 28049 (25 µmol/kg) to C57 BL/6 female mice with murine Colon 38 or Lewis lung tumours ( $n = 3$  per time point)

Tumour	Tissue	AUC (0–∞) (µM h)	$C_{max}$ (µM)	$t_{1/2}$ (h)
Lewis lung	Tumour	216.5 ± 7.2	23.1 ± 0.6	9.3 ± 0.3
	Liver	246.3 ± 13.3	54.1 ± 1.4	4.5 ± 0.2
	Kidney	78.3 ± 2.3	25.5 ± 5.8	5.4 ± 0.4
	Heart	220.1 ± 6.1	45.1 ± 0.2	4.7 ± 0.3
Colon 38 <sup>a</sup>	Tumour	2,334 ± 60	58.4 ± 0.7	17.5 ± 1.5
	Liver	76.1 ± 5.1	39.2 ± 0.8	3.1 ± 0.02
	Kidney	68.7 ± 8.3	22.8 ± 1.8	3.5 ± 0.2
	Heart	87.8 ± 10.8	39.3 ± 1.7	3.7 ± 0.03

Values are expressed as mean ± SEM

<sup>a</sup> From published data [21]

### Comparison of SN 28049 pharmacokinetics in human tumour xenografts

Tissue pharmacokinetic data are shown in Fig. 3, and a comparison of plasma, heart, kidney, liver and tumour pharmacokinetics for the four tumours is shown in Tables 1 and 3. The average AUC values are also compared graphically to the murine tumour data in Fig. 4. The tumour AUC values varied widely from 8.9 µM.h (NZM4) to 321 µM.h (NZM10) and the latter overlapped with the values for the murine tumours.

### Relationship of SN 28049 pharmacokinetics to antitumour activity

In order to compare drug uptake/retention with antitumour activity, the effect of intraperitoneal administration of SN 28049 on growth of subcutaneously implanted tumours in mice was tested. Tumour growth data for the Lewis lung tumour (Fig. 5) indicate that a single drug dose (26.3 µmol/kg) induced a growth delay of 8 days but did not cause a

complete remission, in contrast to the data for the murine Colon 38 tumour [10]. The lower activity in Lewis lung is consistent with the lower tumour tissue AUC (Figs. 2, 4). Three melanoma lines (NZM4, NZM10 and NZM52) were grown as subcutaneous xenografts and treated with SN 28049. Because a dose of 26.3 µmol/kg was toxic to the Balb/c Rag-1 host, two intraperitoneal doses of 17.4 µmol/kg were administered 7 days apart. The NZM4 xenograft showed minimal response to the drug, consistent with its very low tumour tissue AUC. In contrast, the NZM10 xenograft showed a tumour tissue AUC of 321 µM h and was responsive to drug with a tumour growth delay of 12 days. The NZM52 xenograft showed a lower tumour tissue AUC of 99 µM h but showed an even longer tumour growth delay of 35 days (Fig. 5).

### Cellular localisation studies

Preliminary solution studies found that SN 28049 was weakly fluorescent, but that fluorescence was quenched by the presence of DNA. To detect cell-associated SN 28049 in cultured cells, a relatively high drug concentration (10 µM) was required. Studies were carried out using the LLTC and Co38P murine lines and the NZM4, NZM10 and NZM52 human cell lines, using 1 h exposure time. The results (Fig. 6) indicated that all cells showed evidence of drug localisation in cytoplasmic bodies or vesicles.

### Discussion

The results clearly demonstrate that SN 28049 accumulates in vivo to different extents in different tumours. Since two of the tumours are syngeneic while three are xenografts, it is not possible to make complete comparisons. However, as measured by tissue AUC values, the Colon 38 tumour showed a 262-fold higher drug exposure than the NZM4 xenograft, with other tumours showing intermediate values. The tumour AUC values in mice with Colon 38

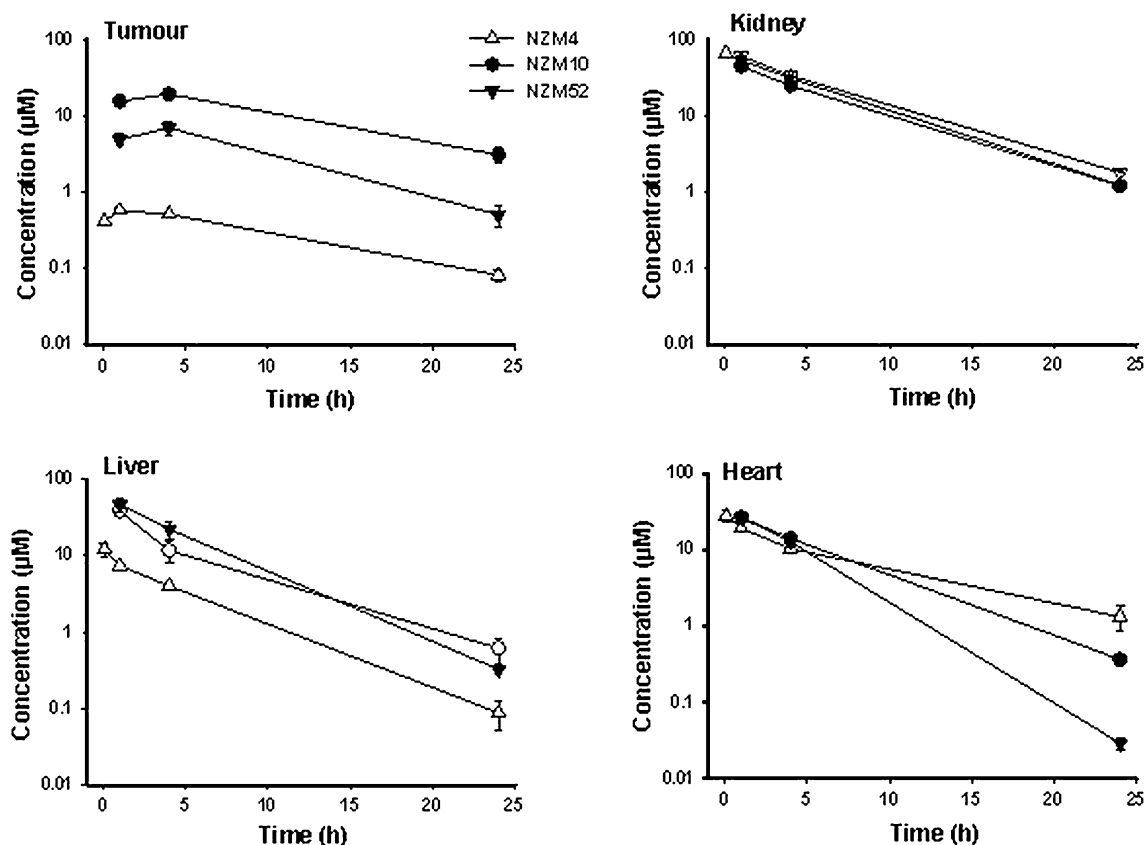


**Fig. 3** Tissue concentrations of SN 28049 (mean  $\pm$  SEM) for tumour, kidney, liver and heart after i.p. drug administration (17.4  $\mu\text{mol/kg}$ ) to tumour-bearing Balb/c Rag-1 female mice ( $n = 3$  per time point)

**Table 3** Tissue pharmacokinetic parameters calculated from concentration–time profiles after i.p. administration of SN 28049 (17.4  $\mu\text{mol/kg}$ ) to Balb/c Rag-1 female mice with NZM4, NZM10 or NZM52 tumour xenografts ( $n = 3$  per time point)

Tumour	Tissue	AUC (0– $\infty$ ) ( $\mu\text{M h}$ )	$C_{\text{max}}$ ( $\mu\text{M}$ )	$t_{1/2}$ (h)
NZM4	Tumour	8.9 $\pm$ 0.3	0.6 $\pm$ 0.03	7.9 $\pm$ 0.3
	Liver	67.5 $\pm$ 2.2	12.1 $\pm$ 1.4	3.6 $\pm$ 0.2
	Kidney	502.0 $\pm$ 41.0	67.3 $\pm$ 6.3	4.3 $\pm$ 0.1
	Heart	183.0 $\pm$ 15.0	27.5 $\pm$ 1.0	4.3 $\pm$ 0.1
NZM10	Tumour	321.0 $\pm$ 34.0	19.1 $\pm$ 2.0	8.8 $\pm$ 0.4
	Liver	220.0 $\pm$ 30.0	38.1 $\pm$ 0.3	4.1 $\pm$ 0.3
	Kidney	441.0 $\pm$ 7.0	44.2 $\pm$ 0.7	4.3 $\pm$ 0.1
	Heart	217.0 $\pm$ 8.0	26.5 $\pm$ 1.0	3.7 $\pm$ 0.1
NZM52	Tumour	99.0 $\pm$ 10.0	6.9 $\pm$ 0.8	6.3 $\pm$ 0.4
	Liver	354.0 $\pm$ 42.0	46.8 $\pm$ 5.9	3.4 $\pm$ 0.1
	Kidney	518.0 $\pm$ 6.0	59.6 $\pm$ 0.8	4.6 $\pm$ 0.05
	Heart	198.0 $\pm$ 6.0	26.3 $\pm$ 1.2	2.3 $\pm$ 0.1

Values are expressed as mean  $\pm$  SEM

and NZM10 tumours were higher than those for the corresponding normal tissues (Tables 2, 3). This was surprising because tumour tissue has a lower vascular density than

normal tissue and a low rate of tissue diffusion, particularly for a DNA-binding drug [22]. For example, a study of the DNA-binding drug doxorubicin in mice bearing the murine Colon 26 tumour showed that the AUC for tumour tissue was 27  $\mu\text{M h}$ , as compared to that for liver (110  $\mu\text{M h}$ ), kidney (207  $\mu\text{M h}$ ) and heart (67  $\mu\text{M h}$ ) [23]. Thus, the normal tissue AUC values for SN 28049 are comparable to those for doxorubicin, but the tumour tissue AUC values are much higher.

Plasma AUC values varied only over a 1.85-fold range for the five tumours (Table 1). Plasma AUC values for C57 BL/6 mice and Rag-1 mice were comparable, even though a lower dose was used for the xenograft study. This is consistent with the lower clearance in Rag-1 mice (Table 1) and the increased drug toxicity in these mice. It was of interest that kidney AUC values for the Rag-1 mice were on average 7.3-fold higher than those for the C57 BL/6 host mice, perhaps reflecting reduced renal clearance (Tables 2, 3). This could be a consequence of the mouse strain difference, including immunodeficiency status. Another feature of the tissue pharmacokinetics was that the presence of a tumour altered the pharmacokinetic profile of normal tissue; the liver tissue AUC in non-tumour-bearing C57 BL/6 mice

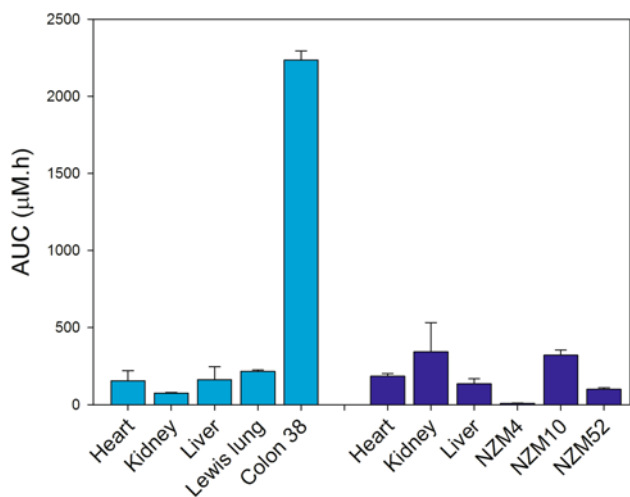


**Fig. 4** **a** AUC values for murine tumours Lewis lung (LLTC) and Colon 38, as well as kidney, liver and heart of tumour-bearing C57 BL/6 mice (25 µmol/kg). Data averaged from Fig. 2. **b** AUC values for xenografted tumours (NZM4, NZM10 and NZM52), as well as kidney, liver and heart of tumour-bearing Balb/c Rag-1 female mice (17.4 µmol/kg). Data averaged from Fig. 3

was  $174 \pm 2.8 \mu\text{M h}$  [13], while that in Colon tumour-bearing mice was significantly lower ( $76.1 \pm 5.1 \mu\text{M h}$ ;  $p < 0.001$ ). A non-tumour-bearing control was not tested in the case of the Balb/c Rag-1 mice, but inspection of the data for the different tumour xenografts shows a range of AUC values in the liver from  $67.5 \pm 2.2$  to  $354 \pm 42 \mu\text{M h}$

(Table 3). Only minor differences were observed for heart and lung tissue pharmacokinetics for the xenograft study, suggesting tissue-selective differences. A possible explanation for this result is that the growth of tumour is known to be associated with increased cytokine activity [24], and cytokines are known to act on liver and other tissues to modulate the activity of drug-metabolising enzymes and drug transporters [25, 26].

Comparison of tumour pharmacokinetics and induced tumour growth delay are difficult, firstly because of widely different tumour growth rates; the approximate volume doubling times for Colon 38, Lewis lung, NZM4, NZM10 and NZM52 tumours were 3.0, 1.0, 12, 5 and 7 days, respectively. Furthermore, the LLTC tumour utilised for the pharmacokinetic studies was a derivative of the Lewis lung tumour used in the growth delay studies and may not respond in the same way. Nevertheless, the lower activity of SN 28049 against the Lewis lung tumour is consistent with a lower tumour AUC, and the lack of activity of SN 28049 against the NZM4 xenograft is consistent with its low tumour tissue AUC (Fig. 4).

It is apparent from the fluorescence images in Fig. 6 that SN 28049 is concentrated in cytoplasmic bodies, probably vesicles, in a manner that have been observed previously with anthracycline antitumour drugs [27]. Further work on the quantitation and time course of drug uptake in cultured cells is in progress. No SN 28049 fluorescence was observed in the nucleus (Fig. 6), but this

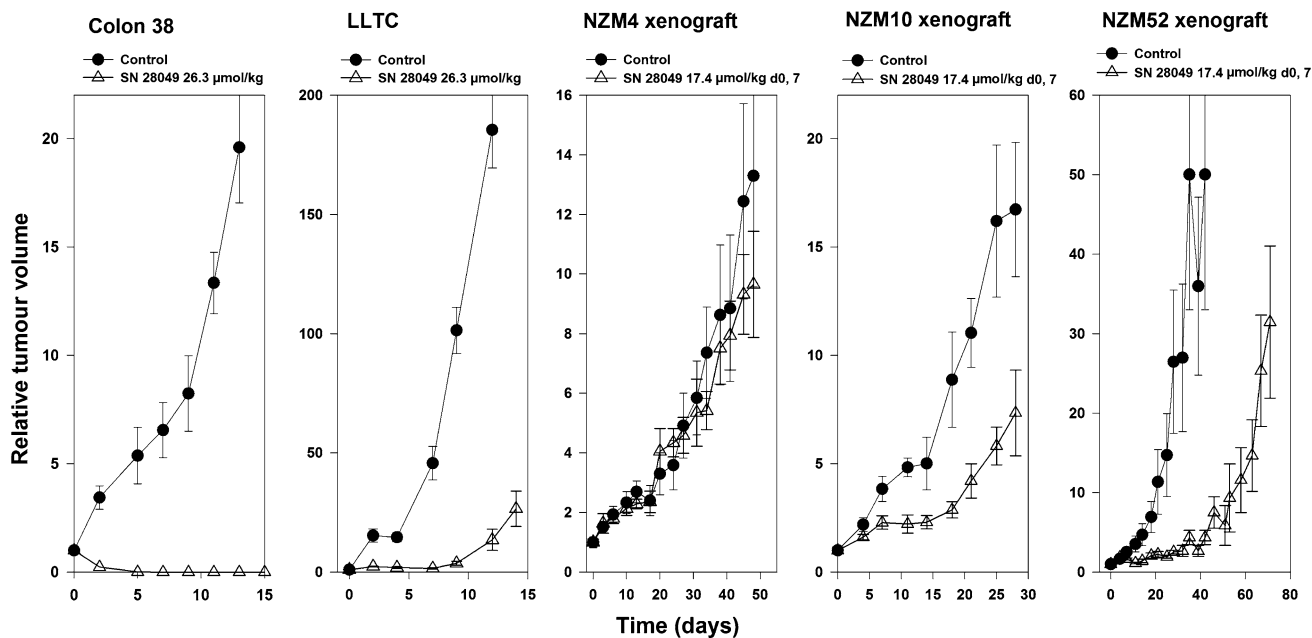


**Fig. 5** Tumour growth delay data. C57 BL/6 mice with Lewis lung murine tumours were treated i.p. with SN 28049 at a single dose (26.3 µmol/kg). Published data for Colon 38 at the same dose [10] are shown for comparison. Balb/c Rag-1 mice with tumour xenografts

(NZM4, NZM10 and NZM52) were treated i.p. with SN 28049 at two doses (17.4 µmol/kg) administered 7 days apart. Vertical bars indicate SEM

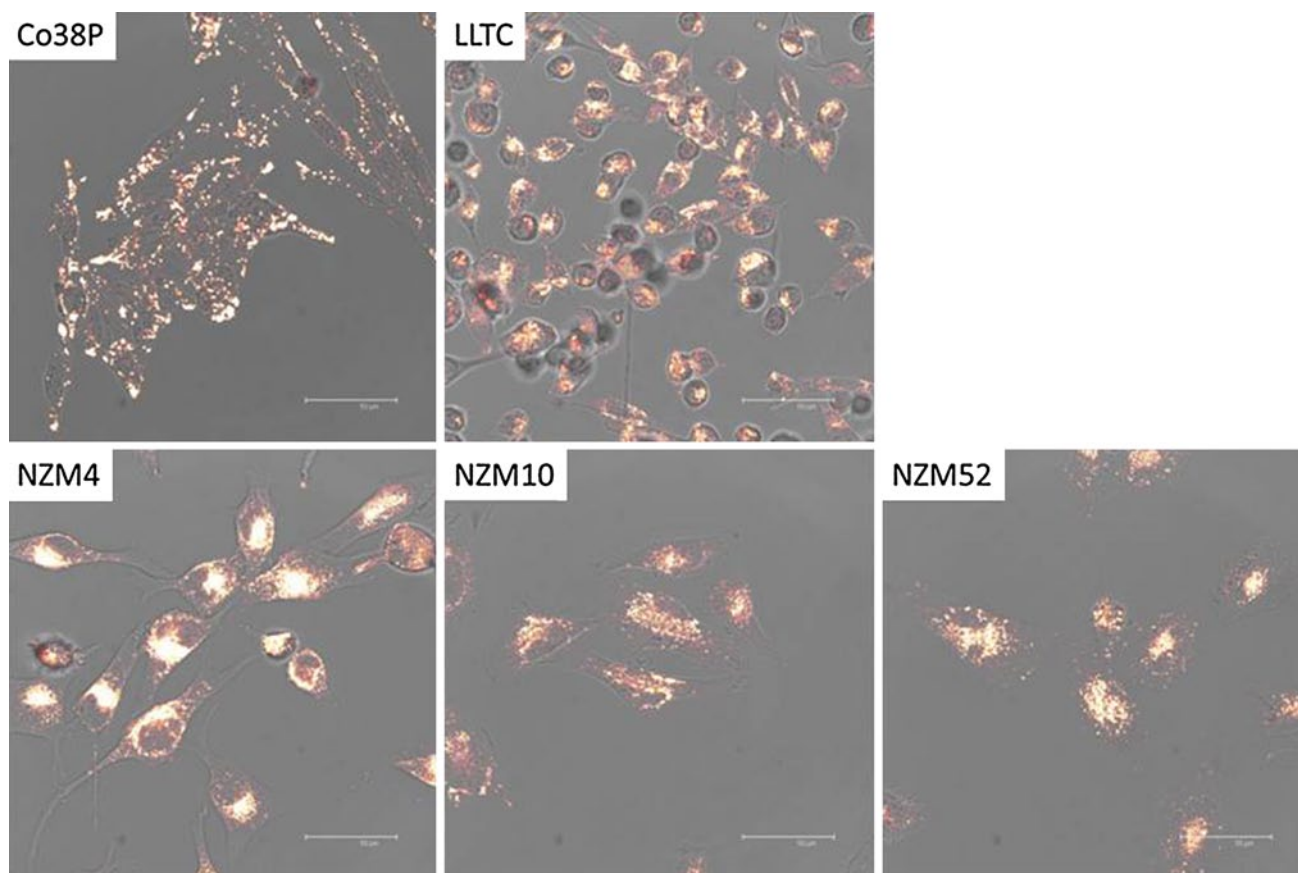


**Fig. 6** Subcellular distribution of SN 28049 in murine (Co38P and LLTC) and human cell lines (NZM4, NZM10 and NZM52), as determined by fluorescence microscopy. Drug images (orange) are overlaid with transmitted light images

is likely to be a consequence of the strong quenching by DNA of SN 28049 fluorescence. Cells were also exposed to doxorubicin, whose fluorescence is not quenched by DNA, and fluorescence was found in both the nucleus and cytoplasm (data not shown), in agreement with reported data [27]. The cytotoxic activity of SN 28049, like that of doxorubicin, is thought to arise from its association with DNA and consequent induction of DNA damage [12]. Hence, the results suggest that SN 28049, like doxorubicin, is present in at least two cellular sites: the nucleus, where DNA-bound drug generates cytotoxicity, and cytoplasmic vesicles, which may contribute to tissue distribution and pharmacokinetics. The results in Fig. 6 show a trend for tumours with the highest tissue-associated drug (AUC) to show the biggest therapeutic response. However, the observed large differences in the concentrations of tissue-associated drug will not necessarily be directly related to cytotoxic activity because of sequestration in the cytoplasm. On the other hand, cytoplasmic drug may also contribute to overall activity by trafficking within the tumour tissue; drug that is eliminated from the cell by exocytosis may be taken up by other cells distal to the blood supply,

thus enhancing drug distribution and lengthening tumour exposure.

The tumour selectivity of topoisomerase II poisons is often regarded as being a function of the cellular enzyme activity, which dictates the degree of drug-induced DNA damage [28]. The present results suggest that tumour-selective cellular uptake mechanisms could play a key role in the selective action of at least some topoisomerase II poisons. A previous study [10] has shown that substitution of the methyl group on the N-2 position of SN 28049 with hydrogen results in an approximately fivefold decrease in growth inhibitory activity in culture but a 330-fold decrease in Colon 38 tumour tissue AUC, underlining the importance of pharmacokinetic factors in activity. The present results indicate that the selective action of SN 28049 is highly tumour dependent, suggesting that drug transport mechanisms may be responsible for this selectivity. It is known that transporters for biological molecules can act on anti-cancer drugs; for instance, the choline transporter has been shown to be involved in the uptake of nitrogen mustard [29], and expression of the carnitine transporter OCTN1 has been shown in a study of the NCI-60 cell line panel



to be a potential transporter for the topoisomerase II poisons doxorubicin and mitoxantrone [30]. Identification of the transporter or other mechanism responsible for tumour-selective retention of SN 28049 would provide the foundation for a treatment strategy in which patients could be selected on the basis of having tumours with a high potential for SN 28049 retention.

**Acknowledgments** This study was supported by the Auckland Cancer Society and by a grant from Auckland UniServices Ltd., New Zealand.

**Conflict of interest** None.

## References

- Nelson EM, Tewey K, Liu LF (1984) Mechanism of antitumor drug action: poisoning of mammalian DNA topoisomerase II on DNA by 4'-(9-acridinylamino)-methanesulfon-m-anisidide. *Proc Natl Acad Sci USA* 81:1361–1365
- Tewey KM, Rowe TC, Yang L, Halligan BD, Liu LF (1984) Adriamycin-induced DNA damage mediated by mammalian DNA topoisomerase II. *Science* 226:466–468
- Arcamone F (1985) Properties of antitumor anthracyclines and new developments in their application: Cain Memorial Award Lecture. *Cancer Res* 45:5995–5999
- Martini A, Donelli NG, Mantovani A, Pacciarini MA, Fogar-Ottaviano EF, Morasca L, Garattini S, Spreafico FS (1977) Antineoplastic activity and pharmacokinetics of adriamycin and daunomycin in tumor bearing mice. *Oncology* 34:173–178
- Arlin ZA (1983) Current status of amsacrine (AMSA) combination chemotherapy programs in acute leukemia. *Cancer Treat Rep* 67:967–970
- Baguley BC, Kernohan AR, Wilson WR (1983) Divergent activity of derivatives of amsacrine (m-AMSA) towards Lewis lung carcinoma and P388 leukaemia in mice. *Eur J Cancer Clin Oncol* 19:1607–1613
- Finlay GJ, Riou JF, Baguley BC (1996) From amsacrine to DACA (N-[2-(dimethylamino)ethyl]acridine-4-carboxamide): selectivity for topoisomerases I and II among acridine derivatives. *Eur J Cancer* 32A:708–714
- Deady LW, Rodemann T, Zhuang L, Baguley BC, Denny WA (2003) Synthesis and cytotoxic activity of carboxamide derivatives of benzo[b][1,6]naphthyridines. *J Med Chem* 46:1049–1054
- Bu X, Chen J, Deady LW, Smith CL, Baguley BC, Greenhalgh D, Yang S, Denny WA (2005) Synthesis and cytotoxic activity of N-[(alkylamino)alkyl]-carboxamide derivatives of 7-oxo-7H-benz[de]anthracene, 7-oxo-7H-naphtho[1,2,3-de]quinoline, and 7-oxo-7H-benzo[e]perimidine. *Bioorg Med Chem* 13:3657–3665
- Deady LW, Rogers ML, Zhuang L, Baguley BC, Denny WA (2005) Synthesis and cytotoxic activity of carboxamide derivatives of benzo[b][1,6]naphthyridin-(5H)ones. *Bioorg Med Chem* 13:1341–1355
- Chen YY, Finlay GJ, Kirker JA, Marshall ES, Richardson E, Baguley BC (2011) In vivo and in vitro assessment of the action of SN 28049, a benzonaphthylidene derivative targeting topoisomerase II, on the murine Colon 38 carcinoma. *Invest New Drugs* 29:1504–1510
- Drummond CJ, Finlay GJ, Broome L, Marshall ES, Richardson E, Baguley BC (2011) Action of SN 28049, a new DNA binding topoisomerase II-directed antitumour drug: comparison with doxorubicin and etoposide. *Invest New Drugs* 29:1102–1110
- Lukka PB, Paxton JW, Kestell P, Baguley BC (2010) Pharmacokinetics and distribution of SN 28049, a novel DNA binding anticancer agent, in mice. *Cancer Chemother Pharmacol* 65:1145–1152
- Lukka PB, Paxton JW, Kestell P, Baguley BC (2012) Comparison of a homologous series of benzonaphthylidene anti-cancer agents in mice: divergence between tumour and plasma pharmacokinetics. *Cancer Chemother Pharmacol* 70:151–160
- Baguley BC, Zhuang L, Marshall E (1995) Experimental solid tumour activity of N-[2-(dimethylamino)ethyl]-acridine-4-carboxamide. *Cancer Chemother Pharmacol* 36:244–248
- Wilkoff LJ, Dulmage E, Chopra DP (1980) Viability of cultured Lewis lung cell populations exposed to beta-retinoic acid (40753). *Proc Soc Exp Biol Med* 163:233–236
- Marshall ES, Finlay GJ, Matthews JH, Shaw JH, Nixon J, Baguley BC (1992) Microculture-based chemosensitivity testing: a feasibility study comparing freshly explanted human melanoma cells with human melanoma cell lines. *J Natl Cancer Inst* 84:340–345
- Marshall ES, Holdaway KM, Shaw JH, Finlay GJ, Matthews JH, Baguley BC (1993) Anticancer drug sensitivity profiles of new and established melanoma cell lines. *Oncol Res* 5:301–309
- Kim JE, Stones C, Joseph WR, Leung E, Finlay GJ, Shelling AN, Phillips WA, Shepherd PR, Baguley BC (2012) Comparison of growth factor signalling pathway utilisation in cultured normal melanocytes and melanoma cell lines. *BMC Cancer* 12:141
- Workman P, Aboagye EO, Balkwill F, Balmain A, Bruder G, Chaplin DJ, Double JA, Everitt J, Farningham DA, Glennie MJ, Kelland LR, Robinson V, Stratford IJ, Tozer GM, Watson S, Wedge SR, Eccles SA (2010) Guidelines for the welfare and use of animals in cancer research. *Br J Cancer* 102:1555–1577
- Lukka PB, Paxton JW, Atwell GJ, Kestell P, Baguley BC (2012) A rapid LC-MS/MS method for the quantitation of a series of benzonaphthylidene derivatives: application to in vivo pharmacokinetic and lipophilicity studies in drug development. *J Pharm Biomed Anal* 63:9–16
- Hicks KO, Pruijn FB, Baguley BC, Wilson WR (2001) Extravascular transport of the DNA intercalator and topoisomerase poison N-[2-(dimethylamino)ethyl]acridine-4-carboxamide (DACA): diffusion and metabolism in multicellular layers of tumor cells. *J Pharmacol Exp Ther* 297:1088–1098
- Shinkai H, Takahashi H, Miyamoto K, Uchida T, Tokiwa T (1996) Comparative pharmacokinetics of KRN8602, a new morpholino anthracycline, and adriamycin in tumor-bearing mice. *Cancer Chemother Pharmacol* 38:417–424
- Balkwill F (2004) Cancer and the chemokine network. *Nat Rev Cancer* 4:540–550
- Morgan ET, Goralski KB, Piquette-Miller M, Renton KW, Robertson GR, Chaluvadi MR, Charles KA, Clarke SJ, Kacevska M, Liddle C, Richardson TA, Sharma R, Sinal CJ (2008) Regulation of drug-metabolizing enzymes and transporters in infection, inflammation, and cancer. *Drug Metab Dispos* 36:205–216
- Fardel O, Le Vee M (2009) Regulation of human hepatic drug transporter expression by pro-inflammatory cytokines. *Expert Opin Drug Metab Toxicol* 5:1469–1481
- Bour-Dill C, Gramain MP, Merlin JL, Marchal S, Guillemin F (2000) Determination of intracellular organelles implicated in daunorubicin cytoplasmic sequestration in multidrug-resistant MCF-7 cells using fluorescence microscopy image analysis. *Cytometry* 39:16–25
- Chikamori K, Grozav AG, Kozuki T, Grabowski D, Ganapathi R, Ganapathi MK (2010) DNA topoisomerase II enzymes as

- molecular targets for cancer chemotherapy. *Curr Cancer Drug Targets* 10:758–771
29. Goldenberg GJ, Vanstone CL, Bihler L (1971) Transport of nitrogen mustard on the transport carrier for choline in L5178Y lymphoblasts. *Science* 172:1148–1149
30. Okabe M, Szakacs G, Reimers MA, Suzuki T, Hall MD, Abe T, Weinstein JN, Gottesman MM (2008) Profiling SLCO and SLC22 genes in the NCI-60 cancer cell lines to identify drug uptake transporters. *Mol Cancer Ther* 7:3081–3091